Journal of Imaging Science and Technology® 51(5): 465–472, 2007.

Digital Fabrication Using High-resolution Liquid Toner Electrophotography

Atsuko Iida, Koichi Ishii, Yasushi Shinjo, Hitoshi Yagi and Masahiro Hosoya▲
Advanced Electron Devices Laboratory, Corporate Research & Development Center, Toshiba Corporation, 1, Komukai-Toshiba-cho, Saiwai-ku, Kawasaki, 212-8582, Japan
E-mail: atsuko.iida@toshiba.co.jp

Abstract. *We have developed a digital fabrication process using high-resolution liquid toner electrophotography, consisting of fine liquid toner, a high-resolution exposure system, and nonelectrical transfer. Fine pitch multiline patterns of Cu wiring can be obtained by printing fine lines with seed toners and by electroless plating deposited on lines. Submicron-diameter seed toners have superfine conductive particles on their surfaces. Adhesion between the seed toner layer and Cu layer was increased by applying surface modification. Multiline patterns of 1 pixel line width (21.6 μm) with the volume resistivity of 2.1×10^{-6} Ωcm were realized by using a 1200 dpi resolution light-emitting diode. Furthermore, the development process of multiline patterns with 2540 dpi resolution was examined by numerical simulations based on the electrophoretic characteristics of liquid toner and on the electrostatic forces. The capability of multiline-pattern formation of line and space (L/S)=10/10 μm was confirmed. The actual toner images of L/S=10/10 μm multiline pattern were obtained by using a 2540 dpi resolution luster scanning unit (LSU). Theoretical and experimental results confirm that the fabrication process using liquid toner electrophotography is available for realizing high-resolution multiline patterns.* © 2007 Society for Imaging Science and Technology.
[DOI: 10.2352/J.ImagingSci.Technol.(2007)51:5(465)]

INTRODUCTION

Fine-pitch-pattern formation of wiring circuit boards and reduction in the cost of manufacturing processes are critically important requirements for electronic components and semiconductor packages. Recently, digital fabrication of electronic components using printing technology has been reported.[1–4] Digital fabrication of circuit boards offers several advantages, notably simple mask-less process, and reduced costs.

We have been developing a high resolution liquid toner electrophotographic imaging technology with the potential to produce fine images equal in quality to those produced by offset printing.[5–13] Extremely high resolution images have been realized by our technology that includes a full color Image-On-Image (IOI) development process, high-resolution LSU with 2540 dpi, and the non-electric transfer process called "shearing transfer".

In this paper, we applied our imaging technology to a new digital fabrication process for an electronic circuit board.[14] The capability of fine line-pattern formation by using liquid toner electrophotographic technology was verified theoretically and experimentally.

HIGH-RESOLUTION LIQUID TONER IMAGING PROCESS

Figure 1 shows a typical configuration of our liquid toner electrophotographic imaging system. It includes a photoreceptor drum, a scorotron charger, an exposure unit, a development unit, a dryer, and a transfer unit at the periphery of the photoreceptor drum. The toner image is dried properly by the dryer on the photoreceptor and is transferred to the intermediate transfer roller by the non-electric transfer process, and then secondary transferred to and thermally fixed on a substrate. The highly efficient performance of the shearing transfer is realized for the drying states in which the toner layer includes the solvent in the range of 5–15 wt %.[7,8]

The searing transfer method is the nonelectrostatic process, which is used in the newly developed liquid toner electrophotograpy.[5–10] The intermediate transfer roller consists of a metal roller with 0.2 mm thick elastic layer of silicone rubber on the surface. The shearing transfer does not depend on an adhesive force of the elastic layer of the intermediate transfer roller. Figure 2 shows a schematic description of the mechanism of this method. In this method, the velocity of the surface of the intermediate transfer roller is slower than that of the surface of the photoreceptor drum by several percent. A distortion occurs in the nip of the elastic layer due to the difference of the velocities, and a

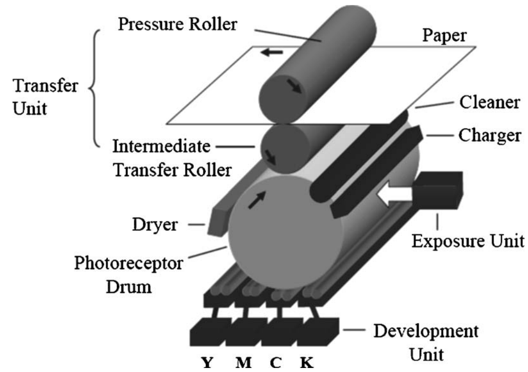

Figure 1. Configuration of liquid toner electrophotographic technology.

▲IS&T Member

Received Mar. 5, 2007; accepted for publication Jun. 7, 2007.
1062-3701/2007/51(5)/465/8/$20.00.

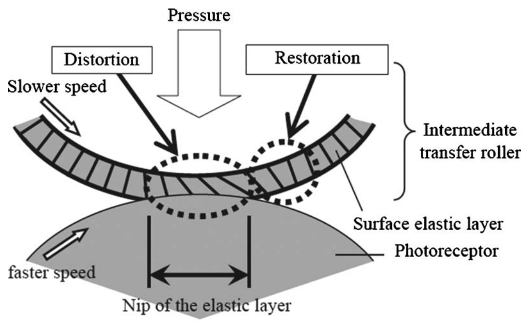

(a)

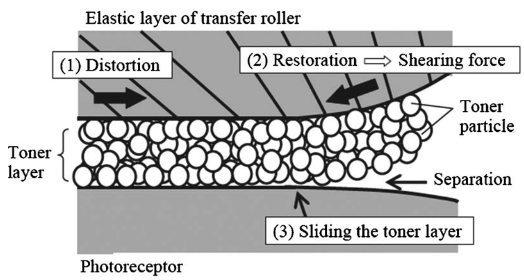

(b)

Figure 2. A schematic of the mechanism of *shearing transfer*: (a) Distortion in the nip area and restoration in the backward of the nip occur by the difference of the velocities. (b) The restoration and friction cause a shearing stress. Shearing stress slides the toner layer on the photoreceptor and transfers it to the transfer roller.

restoration occurs behind the nip [Fig. 2(a)]. The restoration and friction cause a shearing stress between the toner layer and the photoreceptor drum, which slides the toner layer on the photoreceptor and transfers it to the intermediate roller [Fig. 2(b)]. The toner layer moves in unity by the capillary condensation because the toner particles are covered with a thin film of the solvent during the transfer performance.[7,8,15] The method is effective and well directed for a high-resolution image because there is no degradation in quality without toner scattering in an electric transfer method.

Figure 3 shows the comparison of the toner images before and after the transfer process observed by a stereoscopic microscope. The toner image on the paper is in good agreement with that on the photoreceptor surface. The difference of their line widths was observed, but image destruction did not occur due to the transfer. The observation confirms that the shearing transfer method is an excellent method.

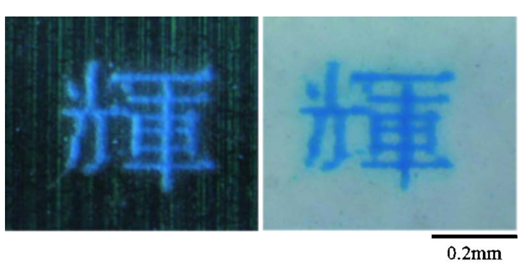

(a) (b)

Figure 3. Comparison of the images before and after the transfer process (2540 dpi, 1 point Chinese character): (a) Toner image before the transfer (on the photoreceptor drum) and (b) toner image after the transfer (on the paper).

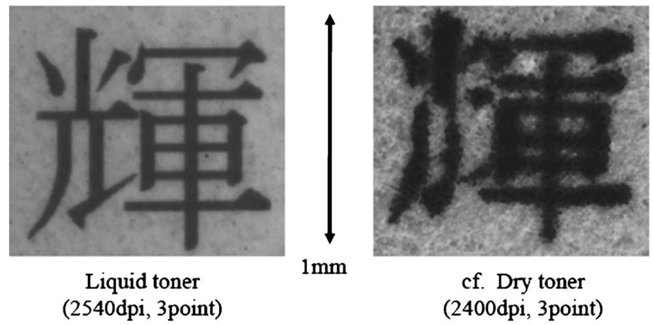

(a)

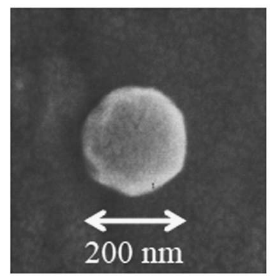

(b)

Figure 4. Printed image obtained by liquid toner electrophotography: (a) Comparison of the printed images on the paper and (b) toner particle.

A printed image realized by our technology is shown in Figure 4(a). Comparison to a printed image realized by dry toner reveals that a finer pitch line was obtained by our technology. Figure 4(b) shows an image of a toner particle observed by a field emission scanning electron microscope (FE-SEM). The average diameter of toner particles was 200 nm.

DIGITAL FABRICATION PROCESS

The digital fabrication process shown in Figure 5 proceeds as follows: first, fine-pitch patterns are printed on the substrate by using seed toners [Fig. 5(a)], and then a surface modification is added on the printed pattern [Fig. 5(b)]. Finally, conductive layers are deposited on the substrate by electroless plating [Fig. 5(c)]. The same electrophotographic system for imaging technology can be used for digital fabrication. Patterns formed on the photoreceptor can be transferred to the substrate, which is almost or partly covered with metallic layers, by using shearing transfer. Silicon wafers, glass, and resin films (such as polyimide, glass epoxy, or polyethylene terephthalate) are used for the substrate.

Image Formation of Fine-pitch Patterns

The basic particle of the seed toner was composed of acrylic thermoplastic resin. The superfine conductive particles were chosen from the metal particles of Ag, Cu, Pd, or any other materials with the catalytic ability to perform as seed for electroless plating. Their average diameters were 20–80 nm. Toner particles prepared by adding a charge controlling agent were dispersed in an insulative solvent, Isopar® manufactured by ExxonMobil Chemical Japan Pte. Ltd.

A positively charged organic photoreceptor with a single coated layer of the phthalocyanine pigment was used. The

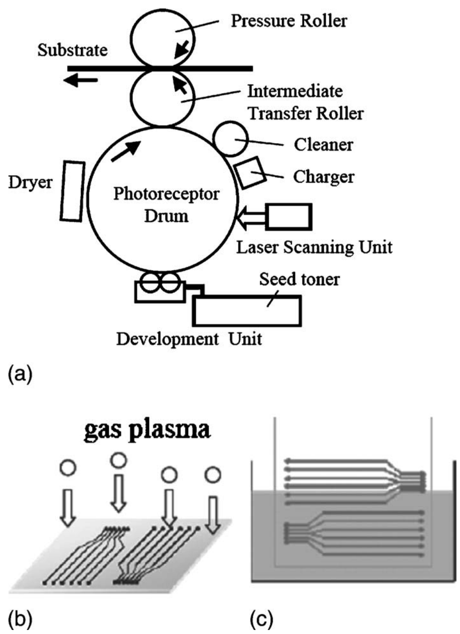

Figure 5. Digital fabrication process: (a) Printing seed toner, (b) surface modification, (c) electroless plating.

photoreceptor drum rotating at a speed of 100 mm/sec was charged uniformly at +700 V by a charger, and a latent image was formed on the photoreceptor by a 1200 dpi LED exposure system. The exposure time was 1.6 μs. Then, the latent image was visualized by a development unit. The voltage applied to the development roller was +550 V. Excess liquid included in the image was removed by a squeeze roller, and the image was dried by an air dryer. Next, the image was transferred to an intermediate transfer roller under pressure of 0.74 MPa at the 100°C without electrostatic forces. The velocity of the surface of the intermediate transfer roller was slower than that of the surface of the photoreceptor drum by 2.5%. Finally, the image was transferred to a substrate under pressure of 0.74 MPa by a backup roller at 100°C.

Fine-pitch pattern of $L/S=1$ pixel/1 pixel (=21.6 μm/21.6 μm) with 1200 dpi resolution was printed on polyimide film as shown in Figure 6. The fine-pitch pattern formed on the photoreceptor surface was transferred to the substrate without deterioration during our transfer process.

In the case of the dry toner electrophotographic system, the toner particle size is $4-8$ μm in diameter.[3,4] The limit of the L/S using dry toner is about 80/80 μm and the line edge shows a ragged shape in the range of several tens of μm. Compared with the dry toner electrophotography, it is possible to achieve higher resolution patterns owing to edge sharpness and to provide higher performance in electroless plating owing to uniform dispersion of conductive particles over the printed pattern. Additionaly, the amount of scattered particles in the vicinity of the line, in the case of using the shearing transfer process, is considerably less than that in the case of using the electric transfer process.

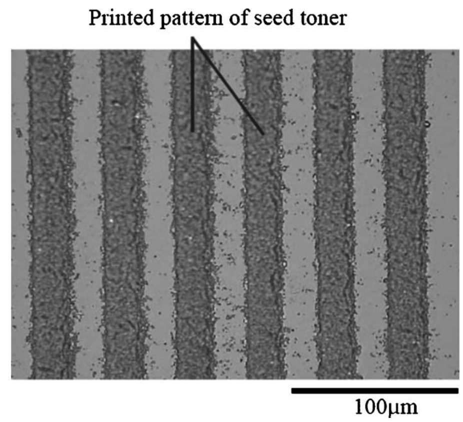

Figure 6. Line/space=1/1 pixel multiline pattern with 1200 dpi exposure system.

Surface Modification after Printing Pattern

Liquid toner imaging technology is advantageous for realizing a flat and smooth surface for printed patterns. However, a surface modification is required in order to successfully use the electroless plating process. The dry etching process was applied to the patterns after printing to form a surface with irregularities. Plasma etch system TE-7500M of Tokyo Electron Ltd. was used for plasma etching with fluorocarbon and oxygen mixture gases. The rate of mixture gases was 1 sccm for C_4F_8 and 10 sccm for O_2, and the total gas pressure was 7.3 Pa. The applied power was 50 W, and etching time was 10 sec. The fluoride deposition was removed by cleaning with HCl solution after plasma etching.

Figure 7 shows the SEM images of the pattern surface, both of as printed [Fig. 7(a)] and after adding surface modification [Fig. 7(b)]. The pattern was printed on the silicon wafer with an insulating coating of epoxy resin film. A slightly rough surface after surface modification is observed, as shown in Fig. 7(b). The resin of the surface was selectively decomposed, and the superfine conductive particles remained after the dry eching process. The weight of the resin decreased by 5%, and the amount of exposed superfine conductive particles increased at the surface.

In the case of the as-printed pattern without any surface modification, however, the Cu film was deposited on it at the initial state of the electroless plating process and the adhesion of the Cu film was insufficient. The deposited Cu film was removed during the electroless plating process. It was not necessary to add the special etching process whenever the line width was more than 50 μm using conductive particles of several hundred nanometers in diameter, the Cu film was deposited successfully without the plasma etching in that case.

The failure of the electroless plating was considered to be attributable to two factors, namely, only a small area of the superfine conductive particles was exposed for electroless plating solution and the "anchor effect" was not obtained sufficiently for the flat surface of the as-printed pattern. Therefore, surface modification as described above was needed before electroless plating.

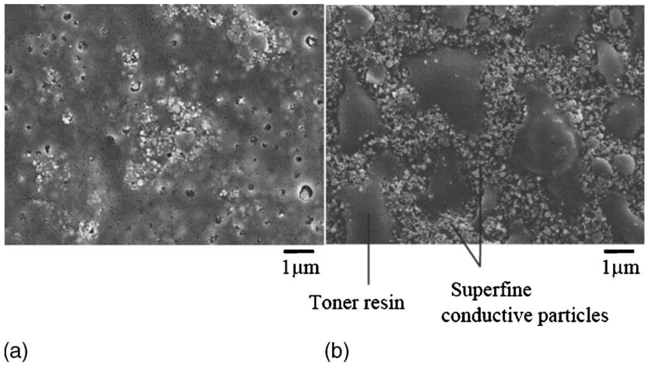

Figure 7. SEM images of pattern surface of seed toner layer: (a) Printed pattern and (b) after surface modification.

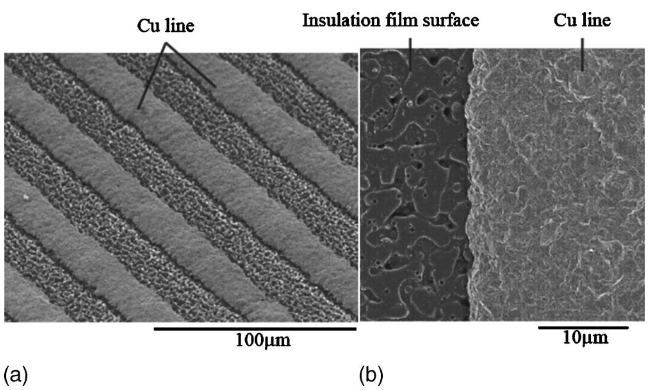

Figure 8. SEM images of $L/S=1/1$ pixel Cu conductive lines. Substrate: Si wafer with insulation film of epoxy resin. (a) Cu conductive pattern and (b) edge of Cu line.

Electroless Plating

Samples were prepared by cleaning in low-concentration acid before electroless plating. The Cu layer was deposited on the printed surface by using a plating solution based on ethylenediamine-tetraacetic acid. Samples were dipped in Thru-Cup ELC-SP®, provided by C. Uyemura & Co., Ltd., at 60°C.

SEM images of Cu conductive pattern are shown in Figure 8. The thickness of the toner layer was $<1\ \mu$m and that of Cu layer was $\sim 3\ \mu$m. Figure 8(b) shows an edge of the Cu line. The raggedness of the line edge was $<2\ \mu$m. Cu lines were clearly isolated from one another. The amount of scattered particles between the printed lines was decreased by applying the surface modification, as shown in Fig. 6. A high-resolution multiline pattern was obtained by using our fabrication process.

Figure 9 shows the SEM cross-sectional view of the Cu line. The cross section of the seed toner layer has fine irregularities whose maximum height (Rz) per reference length λc (where $\lambda c=1\ \mu$m) is 300 nm. The very fine irregularities were obtained by the plasma etching. Adhesion between the seed toner layer and Cu layer was increased dramatically by applying surface modification. No peeling off of the layers was observed during the electroless plating.

The volume resistivity of the Cu line was $2.1\times 10^{-6}\ \Omega$ cm, which is 1.2 times as high as that of bulk Cu. The volume resistivity was slightly higher than that of bulk Cu because the fabrication process was insufficiently optimized in the present study. That is an issue to be tackled in the next phase of this research.

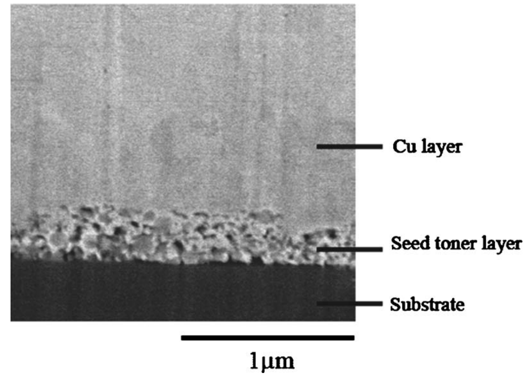

Figure 9. SEM cross-sectional view of Cu conductive line.

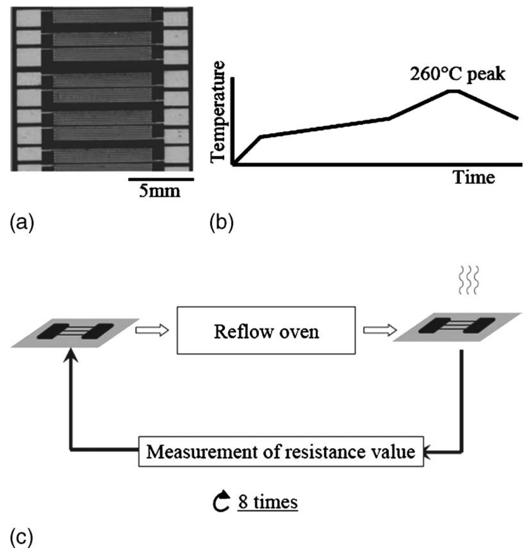

Figure 10. Reliability test: (a) Test pattern ($L/S=2/4$ pixel), (b) reflow oven condition, and (c) reflow test.

Reliability Test

A reliability test was carried out. Change of the resistance of the wiring patterns for $L/S=2$ pixel/4 pixel shown in Figure 10(a) was measured after applying the reflow test. Samples were covered with Au ($t=50$ nm)/Ni ($t=4\ \mu$m) layers by additional electroless plating. The reflow condition was set up for a peak temperature of 260°C, as shown in Fig. 10(b), which is the usual condition for a lead-free solder bump. The reflow test is shown schematically in Fig. 10(c).

Results of the reflow test are shown in Figure 11. The rates of resistance change were <10% for every sample after the reflow test had been performed eight times. The reflow test is severe in the case of the samples including the resin layer. Though the surface of the insulating film was partly decomposed after the reflow test had been performed a few times, the resistance values were stable. The circuits will accordingly be compatible with the conventional bump assembly process.

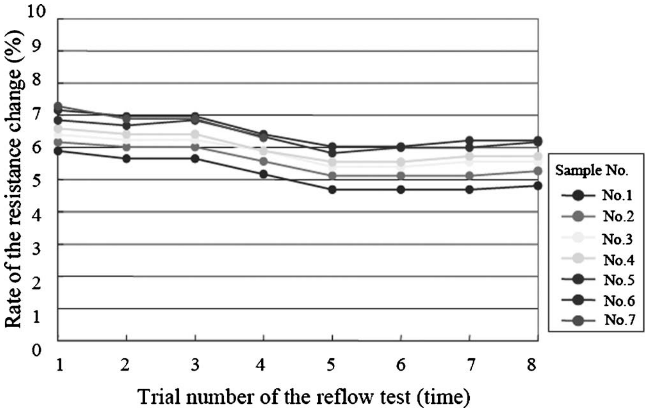

Figure 11. Results of the resistance change after the reflow test.

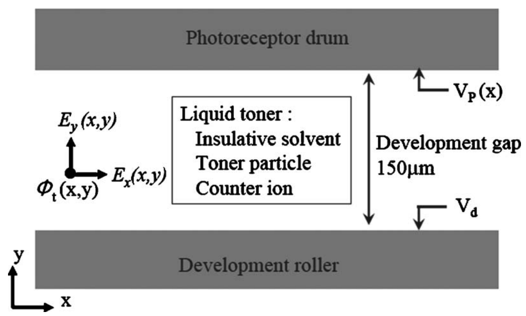

Figure 12. Analysis model of the development area: $V_p(x)$, surface potential distribution of photoreceptor; V_d, development bias; E_x, E_y, electric field in the development area; and $\Phi t(x,y)$, potential distribution in the development area.

Furthermore, for the purpose of examining the capability of multiline-pattern formation using liquid development with a 2450 dpi resolution exposure system, a theoretical analysis is discussed in the next section.

THEORETICAL ANALYSIS OF MULTILINE-PATTERN FORMATION USING LIQUID TONER DEVELOPMENT

In our previous study,[9–13] the high-resolution liquid toner development process of a very fine single dot with 2540 dpi resolution was analyzed theoretically and experimentally. In the present study, the development processes of $L/S=1$ pixel/1 pixel multiline patterns formed with the 2540 dpi resolution exposure system are analyzed.

Analysis Models

An analyzed model is a multiline pattern including ten lines, whose line width is 1 pixel (=10 μm) and space is 10 μm and 20 μm in each case. The development area illustrated in Figure 12 is defined as the rectangle of 300 μm for $L/S=10/10$ μm and 380 μm for $L/S=10/20$ μm, respectively, on the x-axis and 150 μm on the y-axis. The surface potential distributions on the photoreceptor V_p determined from the exposure energy distribution and the photo-induced discharge curve (PIDC) of the positively charged photoreceptor are shown in Figure 13 ($V_0=700$ V, $V_d=400$ V).[9–13,16] However, V_p for $L/S=10/20$ μm were sufficiently isolated from each other, but those for $L/S=10/10$ μm were lower because of the narrow space.

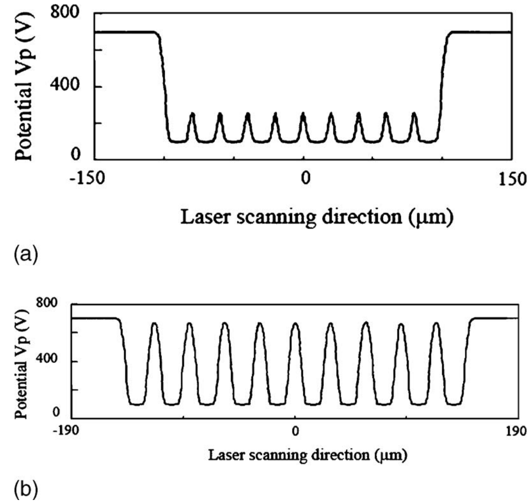

Figure 13. Surface potential distributions V_p of 2540 dpi multiline pattern: (a) $L/S=10/10$ μm and (b) $L/S=10/20$ μm.

Two-Dimensional Liquid Development Model

The toner particles migrate toward the latent image due to the effect of the electric field E originated from the surface potential on the photoreceptor V_p and the development bias V_d. The space and time distributions of the charge density are brought about by the continuity equations [Eqs. (1) and (2)] and Poisson's equation [Eq. (3)].[9–13,17–19] The calculation was performed using differential equations. The charge density of the toner particles ρ_p is positive, and the charge density of the counter ions ρ_n is negative. In the initial state of the development process, both the charge densities, ρ_p and ρ_n, are homogeneous in the area of analysis and their absolute values P_0 are the same. The values used in the analysis are listed in Table I

$$\frac{\partial \rho_p}{\partial t} = -\frac{\partial(\mu_p \rho_p E_x)}{\partial x} - \frac{\partial(\mu_p \rho_p E_y)}{\partial y}, \tag{1}$$

$$\frac{\partial \rho_n}{\partial t} = +\frac{\partial(\mu_n \rho_n E_x)}{\partial x} + \frac{\partial(\mu_n \rho_n E_y)}{\partial y}, \tag{2}$$

$$\frac{\partial^2 \phi_t}{\partial x^2} + \frac{\partial^2 \phi_t}{\partial y^2} = -\left(\frac{\partial E_x}{\partial x} + \frac{\partial E_y}{\partial y}\right) = -\frac{(\rho_p + \rho_n)}{\varepsilon_t}. \tag{3}$$

Table I. Parameters for numerical simulation.

Parameters	Symbol	Value	Unit
Development time	T_d	48	msec
Initial charge density of liquid toner	P_0	1.54	C/m^3
Relative dielectric constant of liquid toner	ϵt	2.03	-
Development gap	dt	150	μm
Mobility of toner particle	μ_p	4.00×10^{-10}	m^2/Vsec
Mobility of counter ion	μ_n	2.00×10^{-10}	m^2/Vsec

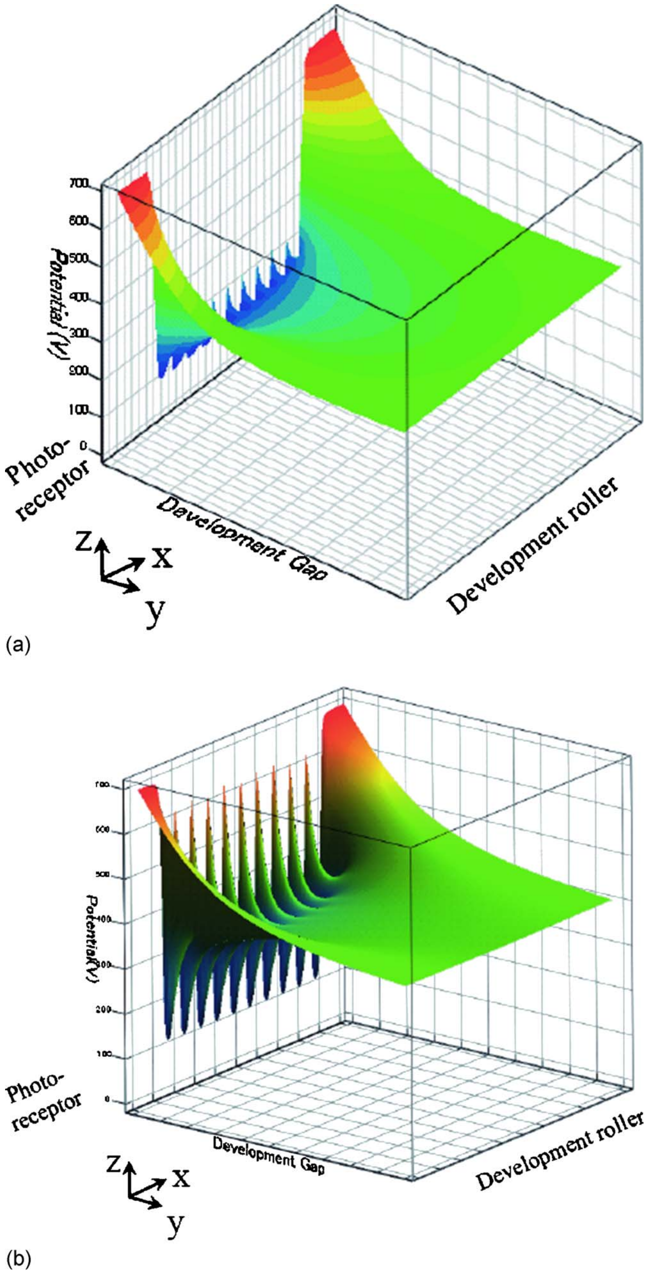

Figure 14. Calculated potential distributions in the development area: (a) $L/S=10/10$ μm and (b) $L/S=10/20$ μm.

Potential and Charge Density Distribution of Multiline Pattern

The calculated potential distributions in the development area for $L/S=10/10$ μm and $10/20$ μm, respectively, are shown three-dimensionally in Figure 14. The x-axis indicates the position in subscanning direction on the photoreceptor surface, and the y-axis indicates the development gap between the photoreceptor and the development roller. It indicates that the potential gradient in the positive direction of y-axis is low except in the vicinity of the photoreceptor surface.

Figure 15 shows the time dependence of toner distribution for $L/S=10/10$ μm. Clear contrast of the charge density was observed in the vicinity of the photoreceptor surface. The multiline pattern formed gradually by migration of

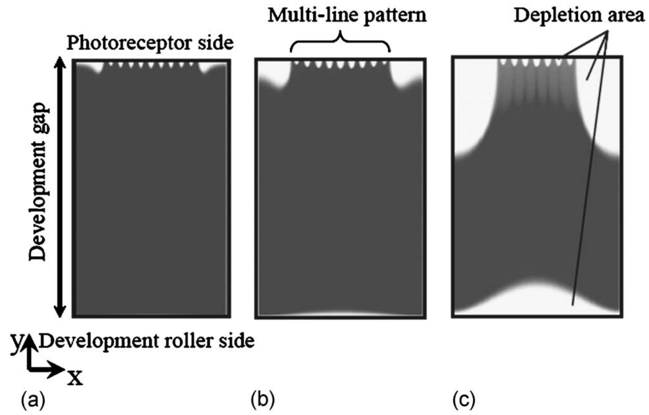

Figure 15. Time dependence of toner distributions for $L/S=10/10$ μm: (a) 1 msec, (b) 5 msec, and (c) 48 msec.

toner particles. Toner particles deposited almost equally on each line in the early stage of the development process ($t=1$ msec). However, toner density of the area outside the multiline pattern decreased rapidly and the depletion area became wider as the development process proceeded. The amounts of deposited toner on both outer lines were less than those of deposited toner on inner lines in the last stage of the development process ($t=48$ msec).

Multiline Formation

Figure 16 shows the L/S dependence of toner distribution in the case of $L/S=10/10$ μm and $10/20$ μm, respectively. Although the surface potential V_p for $L/S=10/10$ μm becomes lower, the lines formed on the photoreceptor are sufficiently isolated from one another.

In this result, the above mentioned "edge effects" were also observed. In particular, the edge effects are rather significant for the fine-pitch mode.

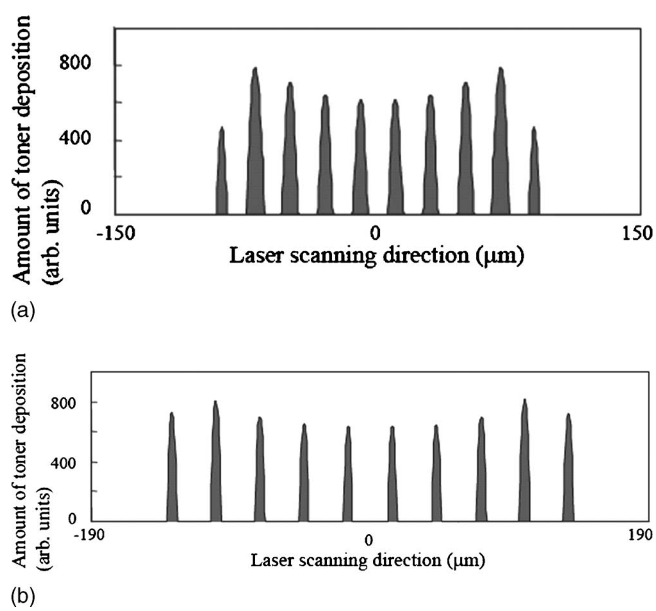

Figure 16. L/S dependence of toner distributions for multiline pattern: (a) $L/S=10/10$ μm and (b) $L/S=10/20$ μm.

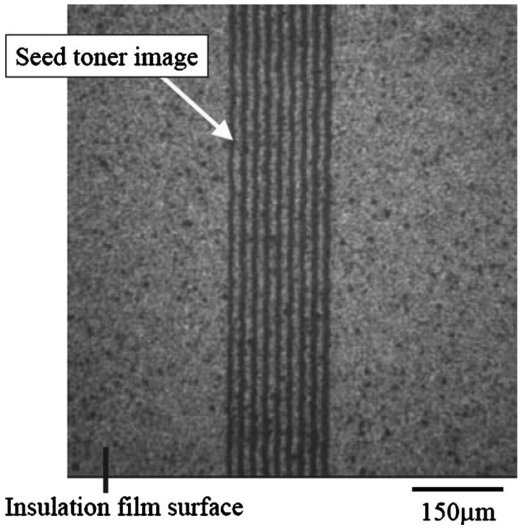

Figure 17. $L/S=10/10$ μm multiline pattern on the Si substrate.

EXPERIMENTAL RESULTS

The seed toner images of $L/S=10/10$ μm multiline pattern were realized by using the real 2540 dpi resolution LSU. Figure 17 shows the lines printed on Si wafer with the insulating coating. Figure 18(a) shows the lines on the polyimide film. Width and height of the lines were measured by laser microscope [Fig. 18(b)]. The edge effect is observed; the amount of deposited toner for the outer line (line No. 1) was less than that of deposited toner for inner lines (Nos. 2–4).

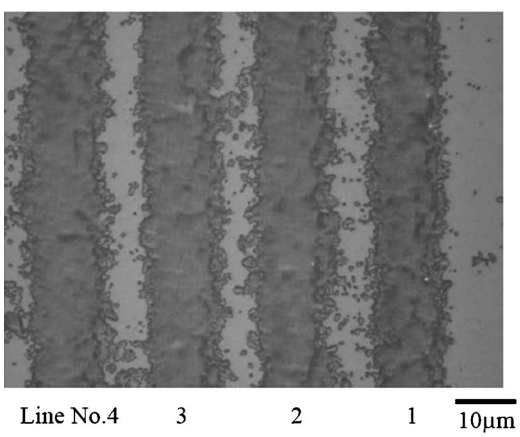

(a)

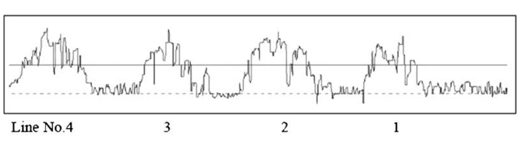

Line No.	1	2	3	4
Width (μm)	10.5	12.3	11.4	11.9
Height (μm)	0.7	0.9	0.8	0.9

(b)

Figure 18. $L/S=10/10$ μm multiline pattern on the polyimide film: (a) Printed pattern on the polyimide film and (b) line shape data measured by laser microscope.

In order to obtain fine multiline patterns with a uniform line width, image processing will be required.

The numerical analysis of fine-pitch multiline patterns agrees well with that of the actual toner images obtained experimentally. We infer that the simulation results precisely describe the actual toner development system.

CONCLUSION

We have developed a digital fabrication process using high-resolution liquid toner electrophotography. The multiline pattern of $L/S=21.6/21.6$ μm was formed by printing the seed toner with a 1200 dpi resolution LED exposure system, and the Cu layer was deposited on the printed lines by electroless plating after surface modification. The liquid toner development of multiline patterns formed with 2540 dpi resolution LSU was analyzed theoretically. The numerical analysis agrees well with the experimental results. These results confirm that the fabrication process using liquid toner electrophotography is available for forming high-resolution multiline patterns.

ACKNOWLEDGMENTS

The authors wish to thank H. Aoki and N. Yamaguchi of Semiconductor Company, Toshiba Corporation, for advice on the assembly technology. They also wish to thank T. Yasumoto and N. Yanase of Semiconductor Company, Toshiba Corporation, for advice on the surface modification. They are grateful to S. Sakamoto and Y. Yamamoto of C. Uyemura & Co., Ltd., for supporting the electroless plating process.

REFERENCES

[1] P. H. Kydd and D. L. Richard, "Electrostatic printing of Parmod™ electrical conductors", *Proc. IS&T's NIP14* (IS&T, Springfield, VA, 1998) pp. 222–225.

[2] P. Calvert, "Inkjet printing for materials and devices", Chem. Mater. **13**, 3299 (2001).

[3] N. Yamaguchi, H. Aoki, C. Takubo, K. Imamiya, T. Yamauchi, and H. Hashizume, "New process using electrophotographic technology for manufacturing printed circuit board", *Proc. ISJ's Japan Hardcopy 2004* (The Imaging Society of Japan, Tokyo, 2004) pp. 121–124.

[4] H. Aoki, N. Yamaguchi, and C. Takubo, "A study of electrophotography process for manufacturing printed circuit board", *Proc. IS&T's NIP20* (IS&T, Springfield, VA, 2004) pp. 241–245.

[5] H. Yagi, Y. Shinjo, H. Oh-oka, M. Saito, K. Ishii, I. Takasu, and M. Hosoya, "Image-on-image color process using liquid toner", *Proc. IS&T's NIP16* (IS&T, Springfield, VA, 2000) pp. 246–250.

[6] S. Hirahara, T. Watanabe, M. Saito, A. Iida, K. Ishii, and M. Hosoya, "Liquid toner image transfer using shearing stress [I]", J. Imag. Soc. Jpn. **42**, 17 (2003).

[7] A. Iida, Y. Shinjo, H. Nukada, S. Hirahara, N. Yoshikawa, and M. Hosoya, "A study of the relationship between drying state of toner and transfer performance in the IOI color process using liquid toner", *Proc. International Congress of Imaging Science 2002* (The Imaging Society of Japan, Tokyo, 2002) pp. 596–597.

[8] A. Iida, Y. Shinjo, H. Nukada, N. Yoshikawa, S. Hirahara, and M. Hosoya, "Relationship between drying state of toner image and transfer performance in the IOI color process using liquid toner", J. Imag. Soc. Jpn. **42**, 24 (2003).

[9] K. Ishii, M. Takahashi, H. Nagato, K. Higuchi, M. Hosoya, and K. Komata, "2540 dpi full color imaging creation with a liquid electrophotography system", *Proc. IS&T's NIP19* (IS&T, Springfield, VA, 2003) pp. 9–12.

[10] K. Ishii, M. Takahashi, H. Nagato, K. Higuchi, M. Hosoya, and K. Komata, "Liquid toner electrophotography for 2540 dpi high resolution image", J. Imag. Soc. Jpn. **44**, 437 (2005).

[11] H. Yagi, Y. Shinjo, H. Oh-oka, M. Saito, K. Ishii, H. Nukada, and M. Hosoya, "Image-on-image color process using liquid toner", J. Imag. Soc. Jpn. **44**, 416 (2005).

[12] Y. Shinjo, H. Yagi, M. Takahashi, K. Ishii, I. Takasu, and M. Hosoya, "Theoretical analysis and experiment of high-resolution development using liquid toner", J. Imag. Soc. Jpn. **44**, 429 (2005).

[13] I. Takasu, H. Yagi, Y. Shinjo, M. Takahashi, and M. Hosoya, "Analysis of 2540 dpi dot reproduction by liquid development", *Proc. IS&T's NIP20* (IS&T, Springfield, VA, 2004) pp. 1027–1031.

[14] A. Iida, K. Ishii, Y. Shinjo, H. Yagi, M. Saito, H. Nukada, M. Takahashi, and M. Hosoya, "A study of digital fabrication using high-resolution liquid toner electrophotography", *Proc. IS&T's Digital Fabrication 2005* (IS&T, Springfield, VA, 2005) pp. 26–29.

[15] J. N. Israelachivili, *Intermolecular and Surface Forces* (Academic Press, New York, 1992).

[16] Y. Kishi, M. Kadonaga, and Y. Watanabe, "Numerical simulation of toner motion in magnetic brush development system", *Proc. ISJ's Japan Hardcopy '99* (The Imaging Society of Japan, Tokyo, 1999) pp. 177–180.

[17] I. Chen, "A charge transport model of liquid development for electrography", J. Imaging Sci. Technol. **39**(6), 473 (1995).

[18] F. J. Wang, G. A. Demoto, H. R. Till, and J. F. Knapp, "Electrophoretic deposition of liquid toners in a plate-out cell—A numerical analysis", *Proc. IS&T's NIP15* (IS&T, Springfield, VA, 1999) pp. 623–626.

[19] S. Aoki, H. Ishida, and G. Takano, "3D toner image simulation considering the latent image formation with laser exposure", *Proc. ISJ's Japan Hardcopy 2003* (The Imaging Society of Japan, Tokyo, 2003) pp. 273–276.